

# GREEN SYNTHESIS AND CHARACTERIZATION OF ZINC OXIDE NANOPARTICLES (ZnO NPs) FROM CAMELLIA SINENSIS LEAF EXTRACT AND ITS POTENTIAL OF ANTIBACTERIAL ACTIVITY AND ACETYL CHOLINESTERASE INHIBITORY ACTIVITIES

## Abstract

Nanoparticles are widely used in the biotechnology and biomedical field. Green synthetic methods of nanoparticles are a simple and environmentally benign process that declines the demerits of conventional chemical and physical methods. The synthesis of semiconductor and metal nanoparticles is a rising research part, due to the possible applications in the progress of new technologies. The present research information the synthesis and characterization of zinc oxide nanoparticles (ZnO NPs) using *C. Sinensis* leaf extract. The findings of these studies show the green synthesized ZnO NPs are effective, safe, and eco-friendly as they are stable and have abundant flower shapes with maximum particles in size ranging from 100 nm in diameter. The synthesized ZnO NPs have been tested against the pathogenic microorganisms and showed an excellent zone of inhibition. DPPH radical scavenging activity of synthesized ZnO NPs expressed DPPH free radicals as a percentage of inhibition and IC<sub>50</sub> value of 70.37%. Acetylcholine esterase (AChE) inhibitory activity possesses the maximum amount of the synthesized ZnO NPs. Since the results of the current work, it was concluded that the synthesized ZnO NPs exhibited significant antibacterial and acetylcholine esterase inhibitory activities. Hence it can be used as a drug with multifunction in treating Alzheimer's disease (AD).

## Keywords

ZnO NPs, antibacterial, FTIR, SEM, *C. sinensis*, AChE

## 1. Introduction

Nanotechnology contains the use of materials having nanoscale size in the range of 1 to 100 nm. In use by nanomaterials have acceptable researchers to have a better understanding of natural science (Santhoshkumaret al., 2017). Nanoscience has been creating a new chemical and biological nanostructure, understanding and uncovering their novel properties and organizing these new structures into larger and more complex functional structures and devices (Prakash and Thiagarajan, 2012). The inorganic nanoparticles (NPs) like gold, silver, copper, TiO<sub>2</sub>, CuO and ZnO have deep antibacterial activities. Among the

inorganic NPs, ZnO NPs are of particular interest, because they can be prepared easily, inexpensive and safe material for human beings and animals. Nanoparticles can be synthesized by various methods like physical (evaporation, condensation and laser ablation), chemical and biological method. Different metal nanoparticles have been synthesized previously using the evaporation-condensation process Deka *et al.*, (2021). They are also generally used in the formulation of health care products. ZnO NPs has entered the scientific spotlight for its high catalytic UV filtering properties, wound healing, anti-bacterial, anti-fungal activity semiconducting properties and photochemical activity (Elumalai and Velmurugan, 2015).

Pharmacology, biotechnology, nanogenerators, biosensors, gas sensors, varistors, solar cells, photo catalysts and photo detectors are capable candidates for a variety of applications ZnO NPs (Talam *et al.*, 2012). ZnO NPs broad applications in pharmacological biological fields. Mainly, metal oxide nanoparticles and ZnO NPs efficiently protects over a broader UV range than any of the molecular UV-absorbers. The non-toxic nature of ZnO NPs makes it fitting in drug research. ZnO NPs are also use as anti-microbials in numerous drugs medicines and formulations (Firdhouse *et al.*, 2015). Toxicological impact of nanomaterials are predictable to relate with the materials of biological components to produce important impacts on the properties and behaviour of body, organs, tissues, cells and macromolecules, cells, tissues, organs and body (Diab *et al.*, 2018). On the increases support of oxidative stress-mediated damages to the lipids, protein and DNA during Alzheimer's disease prompted for the detection of original molecules that play an significant role in cholinesterase inhibitors and scavenging the free radical produced during the pathogenesis of the ailment (Malar *et al.*, 2017).

In this study, the ZnO NPs are synthesized using simple, eco-friendly and cost effective method. The present work is aimed at synthesizing ZnO NPs from leaf extract of *C. sinensis*. The synthesized ZnONP's were characterized by Ultra Visible spectroscopy, Scanning electron microscopy, X-Ray Diffraction, FTIR, Zeta potential and also acetylcholine esterase inhibitory and antibacterial activities of prepared ZnO NPs and tested against different human pathogenic microorganisms (bacteria).

## **2. Materials and Methods**

### **2.1. Materials**

Zinc acetate dihydrate Zn (CH<sub>3</sub>COO)<sub>2</sub>.2H<sub>2</sub>O (M.W 219.49g/mol) were purchased from Isochem Laboratories, Angamaly, Cochin. Catechin (M.W 290.26g/mol) and AChE were

obtained from Sigma-Aldrich Chemical ATCI (M.W 289.18g/mol) and 5,DTNB were obtained from Himedia and all other chemicals were obtained from Himedia which is of analytical grade. Bacterial strains were collected from Microbiological Laboratory Coimbatore, Tamil Nadu.

## 2.2.Plant sample

*C. sinensis* leaves were collected from Aruvankadu in the District of The Nilgiri's, Tamil Nadu, and taxonomic identification of the plant was confirmed by Botanical Survey of India, Coimbatore (Authentication No: BSI/SRC/5/23/2019/Tech./18). The collected plant leaves were kept in shade 10 days for at room temperature for complete drying. The plant material was pulverized and used for further investigations.

## 2.3.Preparation of the plant extract

Aqueous extract: Aqueous extract of *C. sinensis* was prepared according to the method of Kumaret al.(2012). 10 g of thoroughly dried leaves powder were immersed in 100 ml of double distilled water at 60°C for 15 minutes. The extract was filtered using Whatman filter paper and stored at 4°C for further use.

## 2.4. Synthesis and optimization parameters for ZnO NPs

The method proposed by Gnanasangeetha and Thambavani, (2013) was used for the synthesis of ZnO NPs in the selected medicinal plant and the detailed procedure was given in

Figure1.

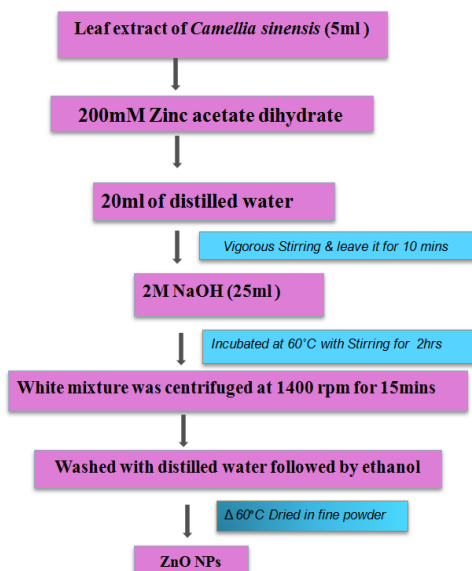


Figure 1: Synthesis of Nanoparticles

Zinc oxide nanoparticles (ZnO NPs) were synthesized using zinc acetate dehydrate  $Zn(CH_3COO)_2 \cdot 2H_2O$ . (modified)briefly, 5ml of leaf extract was taken and 20 ml of 200mM solution of zinc acetate was added. The solution was stirred continuously for 1 hour and then

added 2M NaOH solution (pH 12.0). The mixture was incubated at 60°C with stirring for 2 hours. A white precipitate was centrifuged at 1400 rpm for 5 min and washed twice with sterile distilled water followed by ethanol. Complete conversion to ZnO NPs was then dried to fine powder at 60°C.

## 2.5. Characterization of ZnO NPs

The changed pH of reaction mixture was recorded using digital pH meter during the synthesis of ZnO NPs. UV-Vis spectral analysis was performed using Shimadzu 1800 spectrophotometer, whereas the morphology of the ZnO NPs was observed by SEM with EDAX, Structure and composition of ZnO NPs were analysed by XRD. Further characterization was accomplished by FTIR 2800 Shimadzu and Zeta potential

## 2.6. DPPH radical scavenging activity of synthesized ZnO NPs

The determination of DPPH scavenging activity of the plant extract was done by the method of Kikuzaki and Nakatani (2003). The sample (25µl) and 0.48ml of methanol were added to 0.5ml of methanolic solution of DPPH. The mixture was allowed to react at room temperature for 30 minutes. Methanol alone served as blank and DPPH in methanol, without the plant extracts, served as positive control. After 30minutes of incubation, the discolouration of the purple colour was measured at 518nm. Ascorbic acid was used as a positive control.

The radical scavenging activity was calculated as follows

$$\text{Scavenging activity (\%)} = \frac{A_{518}(\text{sample}) - A_{518}(\text{control})}{A_{518}(\text{control})} \times 100$$

## 2.7. Antibacterial activity of synthesized ZnO NPs

The antibacterial activity of synthesized ZnO NPs was performed by agar disc diffusion method against four bacterial strains (Gram-negative bacteria: *Escherichia coli* MG1655 and *Staphylococcus aureus*, MH605510 Gram-positive bacteria: *Klebsiella oxytoca* 11492-1 and *Bacillus subtilis*. MG859252). All the tested strains were reference strains. The bacterial cultures were grown on nutrient agar medium (Himedia, pH 7.4) at 37°C. The cultures were maintained at 4°C for further use.

The antibacterial activities of synthesized ZnO NPs were screened by agar well diffusion method Tiwari *et al.* (2016). The antimicrobial compounds present in the plant extract are allowed to diffuse out into the medium and allowed to interact in a plate seeded with the test organisms. The diameter of zone of inhibition can be measured in millimetres.

## 2.8. Broth microdilution method

The broth microdilution method was carried out in a 96-well microtiter plate to determine the minimum inhibitory concentration (MIC). The different concentrations of compounds (1, 0.5, 0.25 and 0.125mg/ml) were diluted in Mueller Hinton broth and the final volume was maintained at 100  $\mu$ l. The final concentration of DMSO was less than 1%. From the overnight grown bacterial culture 5  $\mu$ l was added to the test medium to bring the final inoculum size to  $1 \times 10^5$  cfu/ml. The agar plates were incubated at 37° for 16 hour and the absorbance was read at 600 nm. The lowest concentration of the compound that inhibits the complete growth of the bacterium was determined as MIC NCCLS, 2000. The percent growth inhibition was calculated by comparison with a control using the formula indicated below;

$$\% \text{ of growth inhibition} = \frac{\text{control} - \text{test}}{\text{control}} \times 100$$

## **2.9. Thin layer chromatography (TLC) with bioassay detection for AChE inhibition**

The TLC with bioassay detection for AChE inhibition was modified from the study of Rheet *et al.* (2001). A 2.5mm silica gel plate F254 no. 5554 was used as a stationary phase. Two mobile phases, i.e. dichloromethane: ethanol: water 4:4:0.5 (v/v/v) were used. Three microliter of plant extracts dissolved in methanol at concentration of 5 mg/ml was applied to the plate. After the plate had been developed, it was dried at room temperature and then sprayed with 30mM ATCI followed by 20mM DTNB. The plate was dried at room temperature for 45 min, and sprayed with 10.17 U/ml AChE. After 20 min, the plate was observed under visible light. A positive spot indicating AChE inhibitor was a colourless spot on the yellow background. The result was compared to that from the TLC analysis of the same sample after spraying with Anisaldehyde and Dragendorff reagents [14] Dewanjee *et al.*, 2015.

## **2.10. Acetyl cholinesterase inhibition activity**

The acetyl cholinesterase inhibition activity was measured using the method described by Inkanan *et al.* (2003). 3 ml of 50mM Tris-HCl buffer (pH 8.0), 100  $\mu$ l of sample solution at different concentrations (3 mg/ml, 1.5 mg/ml, 0.75 mg/ml) and 20 $\mu$ l AChE (6 U/mL) solution were mixed and incubated for 15 min at 30°C, a 50  $\mu$ l volume of 3 mM 5, 50-dithiobis-(2-nitrobenzoic acid) (DTNB) was added to this mixture. The reaction was then initiated by the addition of 50  $\mu$ l of 15 mM acetylthiocholine iodide (AChI). The hydrolysis of this substrate was monitored at precisely 405 nm wavelength. At this wavelength the formation of yellow 5-thio-2-nitrobenzoate anion was noticed as the result of the reaction of

DTNB with thiocholine, released by the enzymatic hydrolysis of acetylthiocholine iodide. The enzymatic activity was calculated as a percentage of the velocities compared to that of the assay using buffer instead of inhibitor (extract), based on the formula:

$$\text{Enzyme Activity (EA)} = \frac{E-S}{E} \times 100$$

Where, E is the activity of the enzyme without test sample and S is the activity of the enzyme with test sample.

### 2.11. Statistical analysis

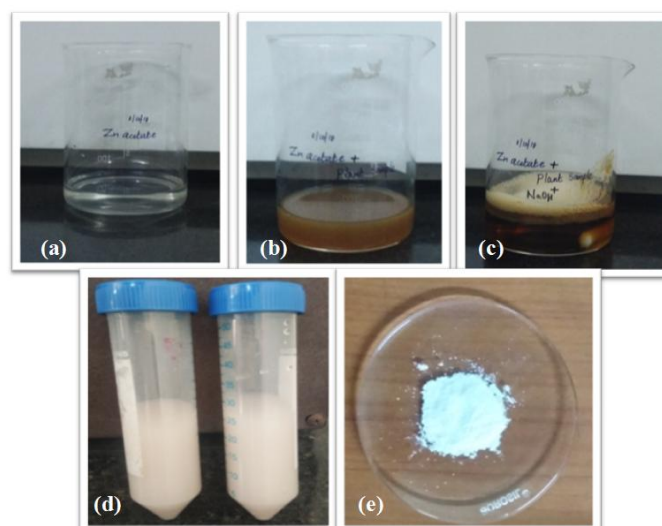
The parameters analyzed of the study were subjected to statistical treatment using SigmaStat Statistical package. All measurements were expressed as mean  $\pm$  standard deviation. Statistical significance was determined by one-way ANOVA. Values of  $p < 0.05$  were considered significant.

## 3. Results and Discussion

### 3.1. Color change

Decrease of zinc is established by color alteration of the reaction mixture from pale yellow to white and shown in Figure 2 and Table 1.

**Figure 2. Color change- synthesized ZnO NPs**



- a) 200 mM zinc acetate (transparent) solution, b) 35 ml of zinc acetate (yellowish white) solution + 15 ml of leaf extract, c) after 6 hours (pale yellow color), d) after 24 hours (white color intensity increased)  
e) Synthesized ZnO NPs

**Table 1: Change in color of solution during formation of synthesized ZnO NPs using leaf extract of *Camellia sinensis***

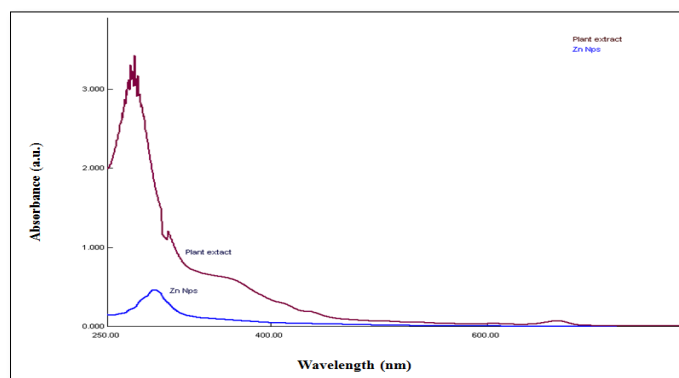
Solution	Reduction		Color intensity	Time
	Before	After		
<i>Camellia sinensis</i> Extract	Light brown	-	-	-
200 mM zinc acetate	Transparent	Pale yellow	+	Immediate
		Yellowish white	++	After 6 h
		White	+++	After 24 h

Visual colour change is the preliminary test for nanoparticles synthesis. For the duration of synthesis, the transform in color of the solution and development of a yellowish-white precipitate was an indication that zinc acetate had been reduced. Similar results was observed by Santhoshkumaret al. (2017), who stated that the ZnO NPs was synthesized using freshly prepared leaf extract of *Passiflora caerulea*.

### 3.2. UV-Vis spectrum of synthesized ZnO NPs

UV-Vis spectroscopy is a significant tool for the determination of development shape and stability of nanoparticles. The UV-spectrum of the synthesized ZnO NPs is shown in Figure 3.

**Figure 3: The UV-Vis spectrum of the ZnO NPs**



**A. Standard B. ZnO NPs**

The spectrum reveals a broad peak which was obtained at wavelength 318nm which can be assigned to the intrinsic band gap absorption of ZnO NPs due to the electron transition from the valence band to the conduction band. The band gap energy of synthesized ZnO NPs is calculated by using formula;

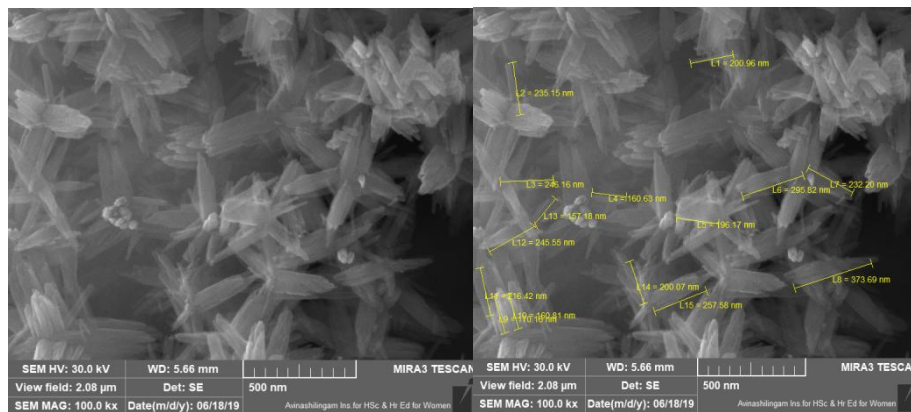
$$E = hc/\lambda$$

Where  $h$  ( $6.626 \times 10^{-34}$  JS) is planks constant  $c$  ( $3 \times 10^8$  m/s) is the velocity of light  $\lambda$  (318 nm) wavelength. The band energy of synthesized ZnO NPs was found to be 3.38 eV. Green synthesis of ZnO NPs was obtained using *Pongamiapinnata* (Suresh *et al.* 2015). The results was in accordance with the Rajeshkumar *et al.* (2018) and confirmed the absorption peak at 380 nm by UV spectrum

### 3.3. SEM analysis of synthesized Zinc oxide Nanoparticles

SEM analysis is through to imagine shape and size of the nanoparticle. The surface morphology of the resulting synthesized ZnO NPs is examined in Figure 4.

**Figure 4: SEM image of synthesized ZnO NPs**



SEM images were seen in different magnification ranges such as 2 μm-200 μm which obviously confirmed the incidence of distinctive and abundant flower shaped ZnO NPs.

**Figure 5: EDAX spectrum of synthesized ZnO NPs**

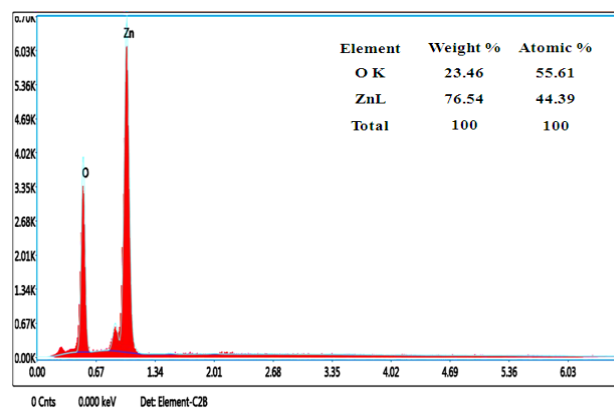


Figure 5 shows the EDAX spectrum of synthesized ZnO NPs. The composition showed from EDAX analysis reveals zinc 76.54% and oxygen 23.36%.

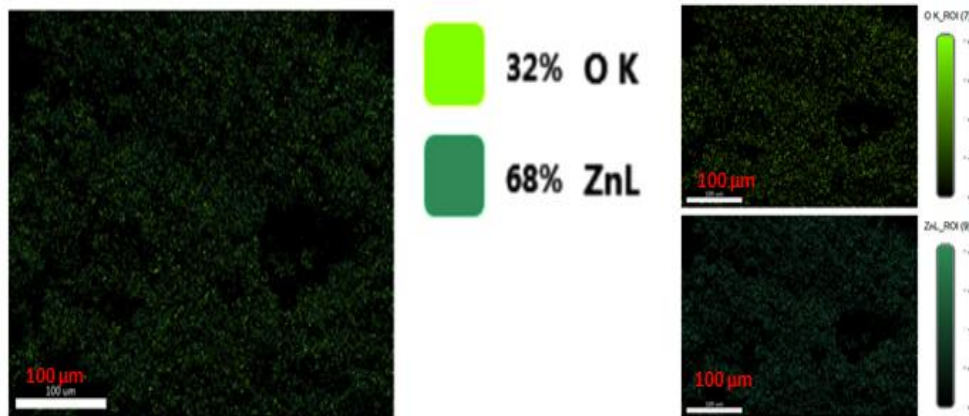
Bala *et al.* (2015) reported that the presence of carbon in trace amount indicates the involvement of plant phytochemical group in reduction and capping of the synthesized ZnO NPs. The results of Rajeshkumar *et al.*, (2018) showed average size of nanoparticles 80 nm

with some agglomerate structures. The synthesized ZnO NPs are in accordance with root extract of *Zingiber officinale* Raja and Jayalakshmy, (2015).

### 3.4. Elemental Mapping analysis of synthesized ZnO NPs

The EDAX spectrum Figure 6 shows only the peaks of zinc and oxygen elements which prove synthesized ZnO NPs.

**Figure 6: Elemental Mapping analysis of synthesized ZnO NPs**



Synthesized ZnO NPs is essentially free from impurities and it is also seen in the limit of EDAX. The Zn and O observed atomic percent value of 23.46 and 76.54 and weight percent value of 55.61 and 44.39 respectively.

### 3.5. XRD patterns of synthesized ZnO NPs

The crystalline size and structure properties of synthesized ZnO NPs are revealed using X-ray diffractions analysis. The XRD carried out with Cu –  $\kappa\alpha$  radiation ( $\kappa = 0.154\text{nm}$ ) and  $2\theta$  range from  $20^\circ$  to  $80^\circ$ . The XRD image of synthesized ZnO NPs is showed in Figure 7. The strong Bragg reflection peaks ( $2\theta = 31.8^\circ, 34.4^\circ, 36.3^\circ, 47.6^\circ, 56.6^\circ, 62.9^\circ, 66.4^\circ$  and  $77.0^\circ$ ) matched by their miller indicates ((100),(002),(101), (102), (110),(103),(112) and (202)) were obtained wurtzite structure (Hexagonal phase) comparison with JCPDS card No: 36-1451 (Aneesh *et al.*,2007) and with JCPDS card No: 89-7102 (Rajiv *et al.*,2013 and Slevarajan & Mohanasrinivasan , 2013).

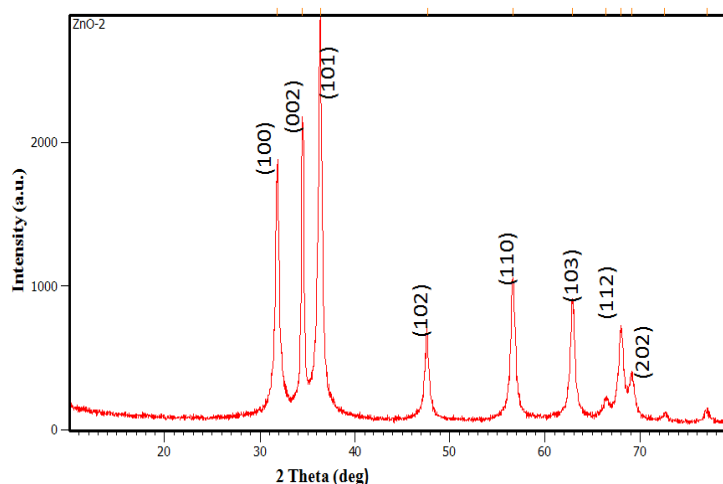
The mean crystallite size (D) of the particles was determined from the XRD line broadening measurement using Scherrer equation

$$D = 0.9\lambda / \beta \cos\theta$$

Where  $\lambda$  is the wave length (Cu –  $\kappa\alpha$ ),  $\beta$  is the full width and half maximum (FWHM) of the ZnO NPs (101) line and theta is the diffraction angle. The calculated crystallite size of

the powder is about 160 nm. Jamdagni *et al.*,(2016) observed that the XRD spectrum crystal lattice indices and particles size calculation of ZnO NPs diffraction peaks were observed at  $2\theta$ . The peaks have been attributed to hexagonal phases of ZnO NPs. The value of particle size was found to be 16.58 nm.

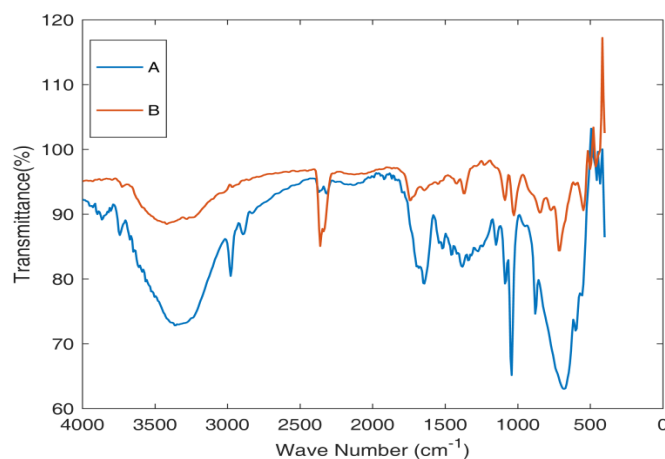
**Figure7: XRD image of synthesized ZnO NPs**



### 3.6.FTIR Spectra of synthesized ZnO NPsanalysis

The FT-IR spectra of *Camellia sinensis* leaf extract before reduction was shown in Figure 8. The absorption bands at  $3390\text{-}3228\text{ cm}^{-1}$  representing O-H stretching alcohol and carboxylic acid. The absorption peak is located at around  $2773\text{ cm}^{-1}$  represented -O-H stretching carboxylic acid stretching vibration present at  $1643$  and  $1701\text{ cm}^{-1}$  are associated with (C=O stretch) vibration of amides and aldehydes respectively. The strong absorption peaks at  $1361$  and  $1226\text{ cm}^{-1}$  which are assigned to  $\text{CH}(\text{CH}_3)_2$  stretching alkanes and alkyls and =C-O- symmetric and asymmetric stretch ethers. Small bands at  $1504$ ,  $929$  and  $821\text{ cm}^{-1}$  represents N-H stretching amides, =C-H- stretching alkanes and C-H stretching vibration of aromatic compounds respectively. After the synthesis of ZnO NPs, FT-IR spectra showed (Figure. 8) strong absorption peaks at  $3441$ ,  $2300$ ,  $1366$ ,  $1026$  and  $709\text{ cm}^{-1}$  which were assigned to -N-H- stretching amines symmetric and asymmetric -O-H- stretching carboxylic acids,  $\text{CH}_3\text{-C-H}$  stretching alkanes and alkyls, C-O stretching alcohol and C-H stretching aromatic compounds respectively. The weaker bands at  $1419$ ,  $1087$ ,  $848$  and  $547\text{ cm}^{-1}$  corresponds to aromatic compounds (-C-C- stretching), alcohol (C-O- stretching), alkenes (=C-H- stretching) and alkyl halides (C-Br- stretching) respectively. The band at  $463\text{ cm}^{-1}$  confirms stretching vibration of ZnO NPs.

**Figure 8: The FT-IR spectra of synthesized ZnO NPs**



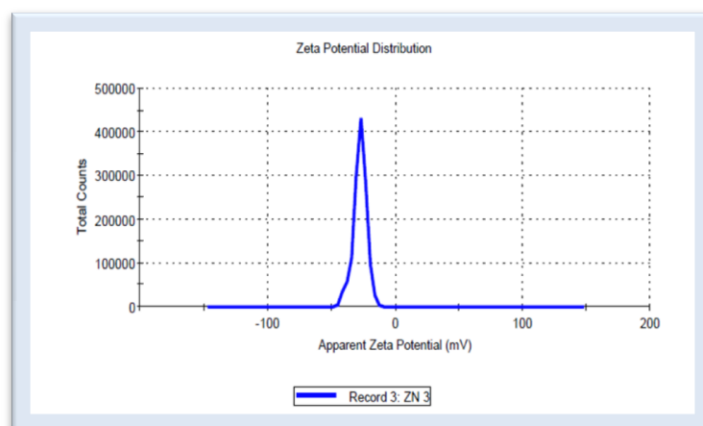
**A. Plantextract      B. ZnO NPs**

Yedurkar *et al.*(2016) demonstrated the presence of C-Alkyl chloride and hexagonal phase ZnO and show peaks at 650.01 and 532.35. Spectroscopy Tutorial 2016 revealed that the 1362.5 peak results from aromatic amines and the 1040 and 1026.65 results from C-N stretch of aliphatic amines. 746.25 and 620.65 peaks correspond to alkanes and supposedly C-H bend in alkynes respectively, hence it confirmed the functional group of zinc oxide nanoparticles.

### 3.7. Zeta potential synthesized ZnO NPs

Zeta potential was used to conclude the surface potential of the synthesized ZnO NPs. Zeta potential is an essential characterization of stability for aqueous ZnO NPs. A minimum of +30 mV Zeta potential is essential for the indication of stable synthesized ZnO NPs. For the showed nanoparticles, zeta values were measured and found to be -11.6 mV with a peak area of 100% intensity. These values present full stabilization of the nanoparticles which may be the main reason in producing particles sizes with a narrow size distribution as shown in Figure 9. The zeta potential of the synthesized zinc oxide nanoparticles was determined in water as dispersant. The high value confirms the repulsion between the particles and thereby increases in stability of the formulation(Yedurkar *et al.*, 2016).

**Figure. 9: The Zeta potential of synthesized ZnO NPs**

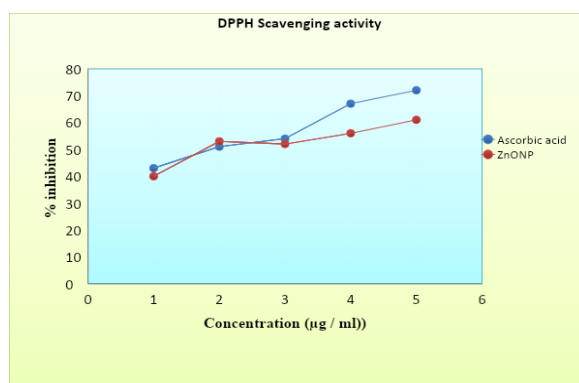


### 3.8. DPPH radical scavenging activity of synthesized ZnO NPs

The inhibition of scavenging activity of synthesized ZnO NPs for DPPH was shown in Figure 10. The inhibition of scavenging activity of the synthesized ZnO NPs was increasing in dose dependent manner and  $IC_{50}$  value of was 70.37%.

Lawrence *et al.*, (2016) observed that the DPPH activity of *Gmelina arborea* extract on radical increased with an increasing concentration of the extract. The  $IC_{50}$  value of the extract was found to be 124.39  $\mu\text{g/ml}$ . Similar results was reported by Mathew *et al.* (2012), showed raw curcumin showed more than 80% DPPH free radical scavenging capacity.

**Figure 10: DPPH scavenging activity of Synthesized ZnO NPs**



### 3.9. Antibacterial activity of Synthesized ZnO NPs

The antibacterial activity against ZnO NPs obtained zones of inhibition growth of the bacteria which varied against test organisms with different concentration ranging from 20 to 80  $\mu\text{l}$  and it is represented in Table 2 and Figure. 11.

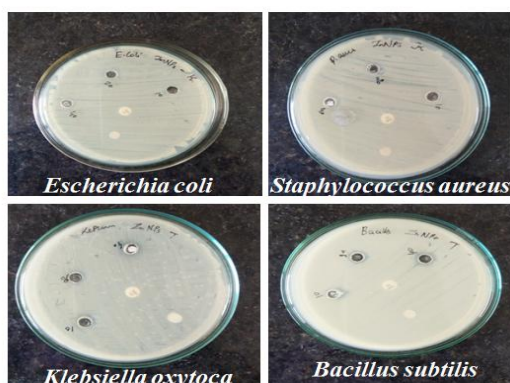
**Table 2. Antibacterial activity of synthesized ZnO NPs  
(Diameter of zone of inhibition in mm)**

Name of the organism	Control	ZnO NPs(mm)
----------------------	---------	-------------

		20	40	60	80
<i>Escherichia coli</i>	0.9	1.6	1.5	1.8	1.5
<i>Staphylococcus aureus</i>	1.3	1.8	1.5	1.3	1.5
<i>Klebsiellaoxytoca</i>	1.5	1.2	1.1	1.2	1.3
<i>Bacillus subtilis</i>	1.1	1.5	1.2	1.4	1.4

The inhibition of zone produced by the sample extract compared with zones produced by ampicillin was used as a control. The results revealed that the ZnO NPs were able to resist against some of the bacterial species. The ZnO NPs showed stronger moderate activity in 50µl concentration against *Escherichia coli* (1.2mm), *Staphylococcus aureus* (0.8mm), *Klebsiellaoxytoca* (0.8mm) and *Bacillus subtilis* (0.9mm).

**Figure 11: Antibacterial activity of synthesized ZnO NPs**



Similar study was reported by Mishra *et al.*, (2015) where the ZnO NPs inhibit the microbial growth. Stan *et al.*, (2015) have also demonstrated that the synthesized Zinc oxide nanoparticles using *Petroselinum crispum* extract showed the microbial growth inhibition which has enhanced 2-16 times when compared with the plant extract.

### 3.10. Determination of minimum inhibitory concentration (MIC)

MIC (Minimum inhibitory concentration) for certain bacteria using synthesized ZnO NPs gave maximum zone in well diffusion method and the results are obtainable in Table 3.

**Table 3. Antibacterial activity of synthesized ZnO NPs against organisms by minimum inhibitory concentration (MIC) method**

Name of the organism	ZnO NPs(mm)			
	20	40	60	80
<i>Escherichia coli</i>	+	-	+	-
<i>Klebsiella oxytoca</i>	+	-	+	-
<i>Staphylococcus aureus</i>	-	-	-	+
<i>Bacillus subtilis</i>	+	-	+	+

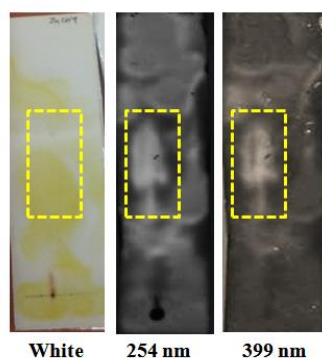
Synthesized ZnO NPs were tested for *Escherichia coli*, *Staphylococcus aureus*, *Klebsiella oxytoca* and *Bacillus subtilis*. The bacterial strains were maintained on nutrient agar at 28°C. MIC value was defined, primarily based upon visual examination bacterial growth in serially diluted nanoparticles suspensions and absence of bacterial growth was visually checked to defined MIC values.

Similar study was reported by Jamdagni *et al.*(2016) and reported that the synthesized ZnO NPs were tested for microbial pathogens and the strains showed the absence of microbial growth was visually checked to define MIC values.

### 3.11. Thin layer chromatography (TLC) with bioassay detection for AChE inhibition

The qualitative results of inhibition of enzyme acetyl cholinesterase in Thin Layer Chromatography showed that synthesized ZnO NPs inhibited the enzyme by the appearance of yellow back ground with white spots was visible after about 5 min. Following are the results of the first test, yellow background with white spots for inhibiting sample and for ZnO NPs were visible after 5 min apparently tested against positive enzyme and gives inhibition at concentration of 5 mg ml<sup>-1</sup> in figure 12.

**Figure 12. TLC qualitative acetyl cholinesterase inhibition (AChEI) assay of ZnONP's**



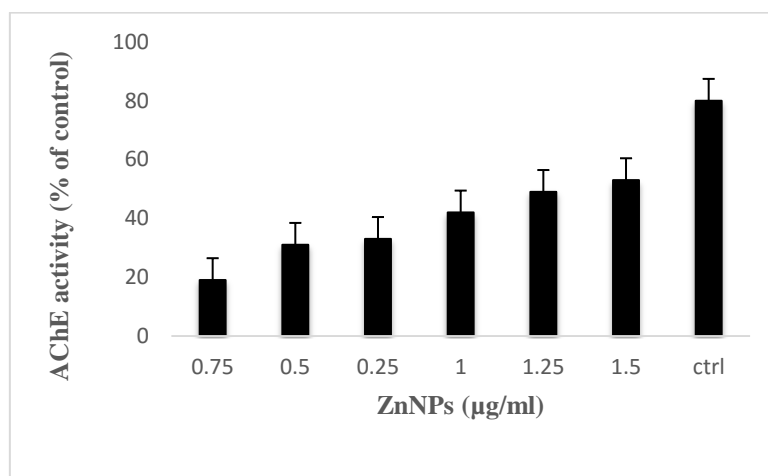
**TLC elutionsystem - dichloromethane: ethanol: water (4:4:0.5 v/v/v).**

*Kalanchoe bra siliensis* extract of 2mg ml<sup>-1</sup> concentration of TLC with white spot showed inhibitory property of cholinesterase with flavonoid compounds (Trevisan *et al.*, 2006). Similar results were obtained by Feitosa *et al.*, (2011) and found that the acetylcholinesterase inhibitors are successfully used to treat the symptoms of Alzheimer's disease.

### 3.12. Acetyl cholinesterase (AChE) inhibitory activity of synthesized ZnO NPs

The percent inhibition data and IC<sub>50</sub> value and Concentration (0.75, 0.50, 0.25, 1, 1.25, 1.5µg/ml) of synthesized ZnO NPs is presented in Figure 13.

**Figure 13: Acetyl cholinesterase (AChE) inhibitory activity of synthesized ZnO NPs**



When studied for its possible inhibitory effect in the *in vitro* analysis, synthesized ZnO NPs showed AChE inhibitory activity in a dose dependent manner with an IC<sub>50</sub> value increasing the extract concentration. Concentration of 1.25 µg/ml in the synthesized ZnO NPs showed the most potent effect in AChE inhibition activity.

Rashed *et al.*,(2015) evaluated anti-alzheimers activity from the isolated compound of 80% methanolic extract of *Ampelopsis brevipedunculata* arial parts.

## 4. Conclusion

The green synthesis of nanoparticles used in this research is found to be non-toxic, eco-friendly, and have less usage of chemicals compared to the chemical and physical methods. The occurrence of phytochemicals in the leaf extract itself helps in the synthesis of metal oxide nanoparticles by inducing oxidation and reduction reactions. The antibacterial activity of synthesized ZnO NPs can be used as a potent antibacterial agent against pathogenic microorganisms and acetylcholinesterase inhibitory activity of ZnO NPs is proved

to be a promising agent of anti-Alzheimer's activity. ZnO NPs are anticipated to have extensive applications in the drug and pharmacology industries.

### **Acknowledgements**

The author thankful to Avinashilingam Institute for Home Science and Higher Education for Women, University, Coimbatore, for providing adequate help required to carry out the work.

### **Conflict of interest**

Authors submitting a manuscript we declared that there are no conflicts of interest in the course of conducting the research. The author has the final decision regarding the manuscript and the decision to submit the findings for publication.

### **References**

Aneesh PM, Vanaja KA, Jayaraj MK, (2007) Synthesis of ZnO nanoparticles by hydrothermal method, Proc. of SPIE Vol. 6639 66390J-1 -8.

Bala N, Saha S, Chakraborty M, Maiti M, Das S, Basu R, Nandy P, (2015) Green synthesis of zinc oxide nanoparticles using *Hibiscus subdariffa* leaf extract: effect of temperature on synthesis, anti-bacterial activity and anti-diabetic activity, RSC Advances.5; 4993-5003.

Dewanjeea S, Gangopadhyayb M, Bhattacharyaa N, Khanraa R, DuaaTK, Bioautography and its scope in the field of natural product chemistry. Journal of Pharmaceutical Analysis., 5(2),75-84.

Diab AA, Ibrahim SSA, Elbahaie ES, Shorbgy IMIE, Abdelhalim WS, (2018)Zinc Oxide Nanoparticles-Induced Neurotoxicity and Possible Mitigating Effects of *Artemisia judaica* and Vitamin C, Research Journal of Pharmaceutical, Biological and Chemical Sciences9(5),519.

Elumalai K, Velmurugan S,(2015) Green synthesis, characterization and antimicrobial activities of Zinc Oxide nanoparticles from the leaf extract of *Azadirachtaindica*(L.), Applied Surface Science1-30.

Feitosa C, De Freitas RM, Luz N, Bezerra M, Trevisan M, (2011) Acetylcholinesterase inhibition by some promising *Brazilian* medicinal plants, Braz.. J. Bio. 71:783-789.

Firdhouse MJ, Lalitha, Vennila P, Biogenic Synthesis of Zinc Oxide Nanoparticles, International Journal of Extensive Research 2,12-20.

Gnanasangeetha D, Thambavani DS, (2014) Facile and eco-friendly method for the synthesis of zinc oxide nanoparticles using *azadirachta* and *emblica*, *International Journal of Pharmaceutical Science and Research* 5(7), 2866-2873.

Ingkaninan K, Temkitthawon P, Chuenchon K, Yuyaem T, Thongnoi W, (2003) Screening for acetylcholinesterase inhibitory activity in plants used in Thai traditional rejuvenating and neurotonic remedies, *Journal Ethnopharmacology*. 89, 261–264.

Jamdagni P, Khatri P, Rana JS, (2016) Green synthesis of zinc oxide nanoparticles using flower extract of *Nyctanthes arbor-tristis* and their antifungal activity, *J King Saud Uni - sci* 1-8.

Kikuzaki H, Nakatani N, (1993) Antioxidant effect of some ginger constituents, *Journal of Food Sciences*. 58, 1407-1410.

Kumar DA, (2012), Rapid and Green synthesis of silver nanoparticles using the leaf extracts of *Parthenium hysterophorus*: A novel biological approach, *International Research Journal of Pharmacy*: 169-173.

Lawrence L, Menon S, Vincent S, Sivaram VP, Padikkala, (2016) Radical scavenging and gastroprotective activity of methanolic extract of *Gmelina arborea* stem bark. *J AyuInte med* 7;78-82.

M., Stan, A., Popa, D., Toloman, T.D., Silipas, D.C., Vodnar, G., Kotona, Enhanced antibacterial activity of Zinc oxide nanoparticles synthesized using *Petroselinum crispum* extracts, *AIP confer. Proce.* 1700 , 0600041 – 0600045, 2015.

Malar DB, Shafreen RB, Pandian SK, Devi KP, (2017) Cholinesterase inhibitory, anti-amyloidogenic and neuroprotective effect of the medicinal plant *Grewia tiliaefolia*- An *in vitro* and *in silico* study. *Pharmaceutical Biology* 55(1), 381-39.

Mathew A, Fukuda T, Nagaka Y, Hasumura T, Morimoto H, Yoshida Y, Maekawa T, Venugopal K, Kumar DS, (2012) Curcumin loaded-PLGA Nanoparticles conjugated with Tet-1 Peptide for potential use in Alzheimer's disease, *Open access Freely available online* 7(3): 1-10.

Mishra V, Sharma R, (2015) Green synthesis of zinc oxide nanoparticles using fresh peels extract of *Punica granatum* and antimicrobial activities, *spectrochimica Acta-part A* 143;158-164.

NCCLS.(National Committee for Clinical Laboratory Standards), (2000) Methods for dilution antimicrobial susceptibility tests for bacteria that grow aerobically; approved standard fifth edition, NCCLS document M7A5, NCCLS, Wayne, PA, USA.

Prakash R, Thiagarajan P. (2012) Synthesis and characterization of silver nanoparticles using *Penicillium sp.* isolated from soil, *International Journal of Advanced Science and Research* 1:138-149.

Raja LFAA, Jayalaksmy E, (2015) A biogenic approach for the synthesis and characterization of Zinc oxide nanoparticles produced by *Tinosporacordifolia*, *Int. J. Pharm. Pharm. Sci.*,7(8), 384-386.

Rajeshkumar S, Agarwal H, Kumar SV, Lakshmi T, (2018) *Brassica oleracea* Mediated synthesis of zinc oxide Nanoparticles and its antibacterial activity against Pathogenic Bacteria. *Asian Journal Chemistry* 30(12), 2711-2715.

Rajiv P, Rajeshwari S, Venckatesh R, (2013) Bio-Fabrication of zinc oxide nanoparticles using leaf extract of *PartheniumhysterophorusL.* and its size-dependent antifungal activity against plant fungal pathogens. *SpectrochimicaActa Part A.*, 112, 384 – 387.

Rashed K, Said A, Feitosa C, Sucupira CC, (2015) Evaluation of Anti-Alzheimer's activity of *Ampelopsis brevipedunculata* and isolated compounds, *Res.JPhytochem.* 9(1);16-24.

Rhee IK, Van der Meent M, Ingkaninan K, Verpoorte R, (2001) Screening for acetylcholinesterase inhibitors from *Amaryllidaceae* using silica gel thin-layer chromatography in combination with bioactivity staining, *Journal of Chromatography* 915, 217–223.

Santhoshkumar J, Venkat Kumar S, Rajeshkumar S (2017) Synthesis of zinc oxide nanoparticles using plant leaf extract against urinary tract infection pathogen, *Resource-Efficient Technologies* 3: 459–465.

Selvarajan E, Mohanasrinivasan V, (2013) Biosynthesis and characterization of ZnO nanoparticles using *Lacto bacillusplantarum* VITES07, *Mat. Let.*, 1-11.

Spectroscopy Tutorial, (2016.) chemistry and biochemistry Department, University of Colorado Boulder  
<http://orgchem.colorado.edu/spectroscopy/specttutor/irchart.pdf> assessed 01.01.16.

Suresh D, Nethravathi PC, Udayabhanu, Nagabhushana H, Rajanaika H, Sharma SC, (2015) Green synthesis of multifunctional zinc oxide (ZnO) nanoparticles using *Cassia fistula* plant extract and their photodegradative, antioxidant and antibacterial activities, *Materials Science in Semiconductor Processing* 31, 446-454.

Talam S, Karumuri SR, Gunnam N, (2012) Research Article Synthesis, Characterization, and Spectroscopic Properties of ZnO Nanoparticles, *International Scholarly Research Network ISRN Nanotechnology* 1, 1-6.

Tiwari M, Roy MR, Tiwari V, (2016) Screening of herbal-based bioactive extract against carbapenem-resistant strain of *Acinetobacter baumannii*. *Microb, Drug Resistance*. 22, 364–371. doi: 10.1089/mdr.2015.0270.

Trevisan MTS, Bezerra MZB, Pinheiro GM, Feitosa CM, Verpoorte R, Filho RB, (2006) Larvicides and acetylcholinesterase inhibitors from *Kalanchoe* species. *New chem.*, 29; 415-424, 2006.

Yedurkar S, Maurya C, Mahanwar P, (2016) Biosynthesis of zinc oxide nanoparticles using *Ixoracoccine* leaf extract – a green approach, *Open J. Synth, Theory Appl.*, 5; 1-14, 2016.

NabaJyotiDeka, Rita Nath, ShantanuTamuly, MousumiHazorika, Seema Rani Pegu and SurjitMoniDeka (2021). Green synthesis and characterization of silver nanoparticles using leaves extract of Neem (*Azadirachta indica L.*) and assessment of its *in vitro* antioxidant and antibacterial activity. *Ann. Phytomed.*, 10(1):171-177. <http://dx.doi.org/10.21276/ap.2021.10.1.17>